Nuclear moments of ^{9}Li

F. D. Correll* and L. Madansky
Department of Physics, The Johns Hopkins University, Baltimore, Maryland 21218

R. A. Hardekopf and J. W. Sunier
Los Alamos National Laboratory, Los Alamos, New Mexico 87545

(Received 17 March 1983)

The ground-state magnetic dipole and electric quadrupole moments of the β emitter ^{9}Li ($J^\pi = \frac{3}{2}^-$, $T_{1/2} = 0.176$ s) have been measured for the first time. Polarized ^{9}Li nuclei were produced in the ^{7}Li($\vec{t}$, p) reaction, using 5–6 MeV polarized tritons. The recoiling ^{9}Li nuclei were stopped either in Au foils or in $LiNbO_3$ single crystals, and their polarization was detected by measuring the β-decay asymmetry. Nuclear magnetic resonance techniques were used to depolarize the nuclei, and the resonant frequencies were deduced from changes in the asymmetry. The ^{9}Li dipole moment was deduced from the measured Larmor frequency in Au; the result, including corrections for diamagnetic shielding and the Knight shift, is $|\mu| = 3.4391(6)\,\mu_N$. The ratio of the ^{9}Li quadrupole moment to that of ^{7}Li was derived from their respective quadrupole couplings in $LiNbO_3$; the value is $|Q(^9\text{Li})/Q(^7\text{Li})| = 0.88 \pm 0.18$. Both results are in agreement with shell model predictions.

[RADIOACTIVITY Polarized ^{9}Li from ^{7}Li($\vec{t}$,p); measured β asymmetry, polarization transfer, NMR; deduced ^{9}Li magnetic moment $|\mu|$, ratio ^{9}Li to ^{7}Li quadrupole moments $|Q(^9\text{Li})/Q(^7\text{Li})|$. Comparison with shell-model values.]

I. INTRODUCTION

Since it was first demonstrated more then twenty years ago,[1] the β-NMR (nuclear magnetic resonance) technique has been used to study the hyperfine interactions of several dozen short-lived β-unstable nuclei. Typically, the first step in such a study is to produce a polarized ensemble of the desired nuclei; then, if their subsequent β decay proceeds by a parity-violating transition, the emission pattern of the decay electrons will be asymmetric with respect to the nuclear spin direction. The second step in the procedure is to observe, by means of this β asymmetry, how the nuclear polarization can be modified by interactions between the electromagnetic moments of the nuclear state and various electric and magnetic fields that are applied to the nuclei. If the properties of the applied fields are known sufficiently well, values of the nuclear moments may be deduced from such observations.

Producing the polarized nuclei for study has often posed a challenging experimental problem. Several methods have been employed, including polarized neutron capture,[1–4] recoil angle selection following nuclear reactions,[5–14] optical pumping,[15–17] and atomic beam spin-state selection.[18,19] Recently, another approach was developed in which beams of polarized protons or deuterons were used to produce and polarize the nuclei of interest in $(\vec{p},n)$,[20,21] $(\vec{p},\alpha)$,[22] $(\vec{d},p)$,[23] or $(\vec{d},n)$ (Ref. 24) reactions. In this method, thick targets are employed which stop all of the recoiling product nuclei, and the desired polarization is achieved by polarization transfer from the beam particles to the final products. Because this polarization transfer is averaged over nearly all possible reaction angles, the net polarization is often rather small. On the other hand, the reaction yield, and therefore the decay-electron counting rate, are usually high, because the target is thick and because all of the reaction products are captured. Furthermore, the degree of polarization obtained in this way is usually rather insensitive to the incident beam energy. Because of these characteristics, the new method is attractive for use in β-NMR measurements.

In this paper, we report the first use of a polarized triton beam in an experiment of this type, resulting in the first measurement of the ground-state nuclear moments of the β emitter ^{9}Li ($J^\pi = \frac{3}{2}^-$; $T_{1/2} = 0.176$ s). Polarized ^{9}Li nuclei were produced in their ground state using the ^{7}Li($\vec{t}$,p)^{9}Li reaction initiated by polarized tritons of 5–6 MeV incident energy. The nuclei were stopped either in polycrystalline Au foils or in single crystals of $LiNbO_3$, and their polarization was preserved for periods of time comparable to their half-life by applying a static magnetic field of approximately 1 kG over the region of the stopping material. Nuclear magnetic resonance measurements were made on the ^{9}Li nuclei implanted in the Au, from which a value for the ^{9}Li ground state magnetic moment was deduced. In addition, from NMR studies of ^{9}Li implanted in the single-crystal $LiNbO_3$, an estimate of the quadrupole coupling in that lattice was made. This was combined with the previously measured coupling of ^{7}Li in $LiNbO_3$ to yield an estimate of the quadrupole moment ratio $|Q(^9\text{Li})/Q(^7\text{Li})|$. Both experimental values were found to be in reasonable agreement with shell model predictions. A detailed description of the experiment is contained in Ref. 25; preliminary results were reported in Ref. 26.

II. THEORY OF β-NMR ON ^{9}Li

A. β emission from polarized nuclei

The emission pattern of decay electrons from a polarized ensemble of β-unstable nuclei is described by[27]

$$W(\theta)=1+\frac{v}{c}AP\cos\theta\ , \tag{1}$$

where P is the nuclear polarization of the ensemble; θ is the angle between the electron momentum and the spin quantization axis (in this case, the direction of the applied magnetic field); v and c are, respectively, the velocities of the electron and of light; and A is an asymmetry parameter whose value ($|A|<1$) depends upon the properties of the particular β decay under consideration.

In the case of ^{9}Li, it is not possible to specify a single asymmetry parameter, because there are three β decay branches. These lead from the ^{9}Li ground state ($J^\pi=\frac{3}{2}^-$) to one of three final states in ^{9}Be: the ground state ($J^\pi=\frac{3}{2}^-$), the 2.43-MeV level ($J^\pi=\frac{5}{2}^-$), or the 2.78-MeV level ($J^\pi=\frac{1}{2}^-$) with branching ratios of $65.0^{+2.7}_{-2.4}$%, $32.0^{+2.7}_{-3.7}$%, and $3.0^{+2.7}_{-0.3}$%, respectively, as illustrated in Fig. 1.[28] On the basis of their measured ft (or comparative half-life) values, these decays have all been identified with pure Gamow-Teller transitions.[29] For each such transition, the asymmetry parameter is given[27] by a simple expression involving only the initial and final nuclear spins, J_i and J_f, as shown in Table I. Thus, the asymmetry parameters associated with the three decay branches of ^{9}Li are -0.40, 0.60, and -1.0, respectively.

In the event that all of the decay electrons detected by the experimental apparatus have values of v/c that are close to unity, an "effective" asymmetry parameter, A_{eff}, for the experiment may be calculated by averaging the values for the individual branches weighted by the respective branching ratios. The result of a simple calculation, in which the quoted uncertainties in each measured branching ratio are replaced by symmetrical uncertainties equal to the larger of the quoted values, is

$$A_{\text{eff}}=-0.098\pm0.022\ .$$

This calculation serves mainly to indicate that the effective asymmetry parameter for the experiment is small, so that rather small β asymmetries should be expected, as discussed further in the next section.

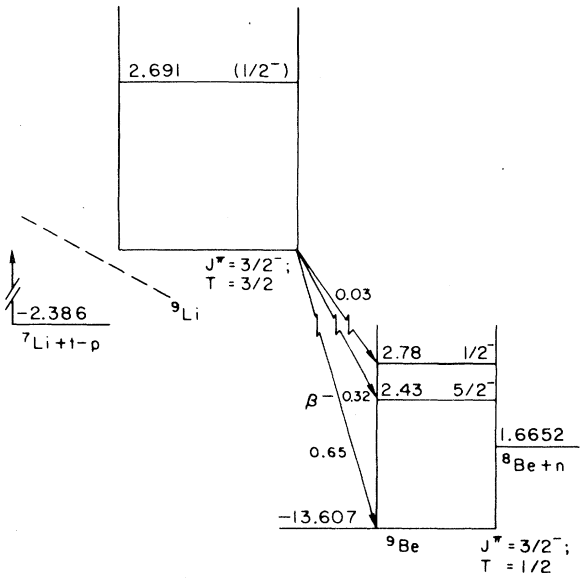

FIG. 1. Beta decay modes and branching ratios for ^{9}Li.

TABLE I. Asymmetry parameter A for allowed Gamow-Teller beta transitions. (Upper sign pertains to electron decay.)

J_i,J_f	A
$J_f=J_i+1$	$\pm\frac{J_i}{J_i+1}$
$J_f=J_i-1$	∓1
$J_f=J_i$	$\mp\frac{1}{J_i+1}$

B. Measurement of the β asymmetry

A convenient experimental measure of the β asymmetry is the quantity $\epsilon=(r-1)/(r+1)$, where

$$r=\left[\frac{N_U(0°)N_D(180°)}{N_U(180°)N_D(0°)}\right]^{1/2}\ .$$

In this expression, $N(0°)/N(180°)$ is the ratio of numbers of decay electrons detected in directions parallel (0°) and antiparallel (180°) to that of the applied field. This expression for r contains two such ratios: one evaluated when the unstable nuclei are produced with tritons whose spins are "up" (U), or parallel to the field, and another evaluated for tritons whose spins are "down" (D), or antiparallel. Dividing one ratio by the other cancels false asymmetries that might otherwise arise from geometrical effects or differences in detector efficiency.

The number $N(\theta)$ is proportional to the emission probability $W(\theta)$ integrated over the solid angles of the detector system. If $W(\theta)$ is assumed to be nearly constant over those solid angles, and if in addition the nuclear polarization P is assumed to be constant in time but of opposite sign for opposite directions of the incident triton spin, the value $\epsilon=PA$ may be computed from these expressions. That is, under these idealized conditions, the expected value of the β asymmetry is equal to the product of the nuclear polarization and the asymmetry parameter. In fact, the measured β asymmetry should be expected to be smaller than this product, for several reasons. First, the nuclear polarization P of the product nuclei may not be perfectly preserved as these nuclei are brought to rest in the stopping medium. Additionally, $W(\theta)$ always varies somewhat over the acceptance angles of the detectors, and the nuclear polarization usually relaxes slightly during the time of the measurment. Finally, beta-unstable nuclides other than the ones of interest may be produced, and these will generally be unpolarized. All of these effects tend to reduce the measured β asymmetry for a given initial polarization of the nuclei under study, so that the value $\epsilon=PA$ should be regarded simply as an upper limit on the asymmetry that will be observed. From another point of

view, the polarization computed from the measured asymmetry and the calculated asymmetry parameter should be regarded as a lower limit on the polarization produced in the reaction.

C. Basis of the β-NMR technique

In the β-NMR technique, standard NMR methods are used to induce transitions between the various magnetic substates of the unstable nuclear state being studied. These transitions change the polarization of the ensemble and, therefore, the observable β asymmetry. The resonant frequencies at which these transitions occur depend upon the hyperfine interaction energies of the nuclear moments and the fields acting on the nuclei. In certain cases, measurements of the resonant frequencies and knowledge of the properties of the hyperfine fields permit one to extract values for the nuclear moments of the state.

One especially important case is that of a collection of nuclei in a state with spin J at rest in a static magnetic field H_0. These conditions exist, for example, if the unstable nuclei are stopped in lattices of cubic metals such as Au, where the lattice symmetry ensures that (except for small corrections) only the applied field H_0 acts on the nuclei. The Zeeman interaction then splits the nuclear state into $2J+1$ magnetic substates, whose energies, relative to their common energy in the absence of an applied field, are ${}^{30}E_m = -mg\mu_N H_0$, where $g = \mu/J$ is the nuclear g factor of the state and μ is its magnetic dipole moment in units of the nuclear magneton μ_N. This arrangement of substate energies is illustrated on the left-hand side of Fig. 2(a).

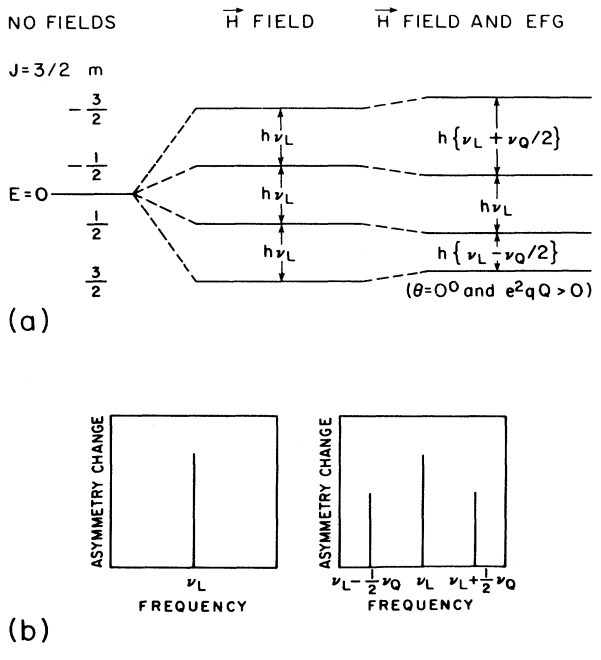

FIG. 2. (a) Energy spacings of the magnetic sublevels of a state with $J=\frac{3}{2}$ in the presence of a magnetic field alone (center) and a magnetic field plus an electric field gradient (right). (b) Expected variation of the beta asymmetry as a function of the perturbing field frequency for the two cases illustrated above.

Given an initially polarized collection of such nuclei, transitions can be induced between the various substates, equalizing the populations and destroying the polarization. This is accomplished by applying a time-dependent perturbation, usually a weak, oscillating magnetic field H_1 whose direction is perpendicular to that of the static field and whose frequency can be varied and precisely measured. The most probable transitions occur between adjacent substates ($\Delta m = \pm 1$) when a single quantum, whose energy $h\nu$ is equal to the splitting between those substates, interacts with a nucleus. For the pure Zeeman interaction, this splitting is the same for all pairs of adjacent substates, and is equal to $\Delta E = |g|\mu_N H_0$. Consequently, the resonant condition is $h\nu_L = |g|\mu_N H_0$, where ν_L is the familiar Larmor frequency of the unstable nucleus in the field H_0. Measurements of the field strength H_0 and the frequency ν_L at which the depolarization is observed permit a precise evaluation of $|g|$. Note that the sign of g cannot be determined using this simple experimental technique. If information concerning the sign of g is required, a more sophisticated approach using circularly-polarized perturbing fields may be employed, but this was not done in the present experiment.

The expected change in β asymmetry as a function of the perturbing-field frequency is shown schematically for the case of the pure Zeeman splitting on the left-hand side of Fig. 2(b). The magnitude of the change depends upon the initial populations of the substates, which determines the initial nuclear polarization, and also upon the induced transition probability, which determines the final polarization. Although the asymmetry change is illustrated in Fig. 2 as an infinitely sharp function of frequency, a number of effects, including instrumental resolution and interactions between the unstable nuclei and the stable lattice nuclei, contribute to produce a resonance line of considerable width.

A more complex pattern of substate energies results if the nuclear state of interest possesses an electric quadrupole moment and if the stopped nuclei experience an electric field gradient (EFG) in addition to the static magnetic field H_0. This can be arranged by stopping the nuclei in a material such as $LiNbO_3$, whose crystal lattice has hexagonal,[31] rather than cubic, symmetry.

Perturbation theory can be used to calculate the effect of the quadrupolar interaction on the energies of the magnetic substates, assuming the strength of the interaction is small compared to the Zeeman splitting. The result, for axially-symmetric EFG's such as those at Li-atom sites in $LiNbO_3$,[32,33] is[34]

$$E_m = -mg\mu_N H_0 + \frac{e^2qQ}{8J(2J-1)}(3\cos^2\theta - 1) \times [3m^2 - J(J+1)] , \quad (2)$$

where eq is the magnitude of the EFG, Q is the electric quadrupole moment of the state, and θ is the angle between the crystalline symmetry axis (the c axis) and the direction of the external field H_0.

In this case, the energies of adjacent substates differ by amounts that depend upon which pair of states is being considered:

$$\Delta E = E_m - E_{m-1} = g\mu_N H_0 - \frac{3e^2qQ}{4J(2J-1)} \times (3\cos^2\theta - 1)(m+\tfrac{1}{2}) . \quad (3)$$

As a result, different resonant frequencies exist for single-quantum transitions induced between different pairs of states, and also for different orientations of the crystal with respect to the external magnetic field.

In the experiments reported here, the crystals were fixed with the c axis always parallel to the external field ($\theta=0°$). A better procedure would be to make a series of measurements with different crystal orientations, so that the orientation dependence of the resonant frequencies could be verified. Such an approach can be very time consuming, however, and it was not attempted.

The substate energies for the case of $\theta=0°$ are illustrated on the right-hand side of Fig. 2(a), where the additional assumption that $e^2qQ>0$ has been incorporated. Explicit expressions for the single-quantum resonant frequencies under these conditions are

$$E(-\tfrac{1}{2}\leftrightarrow+\tfrac{1}{2}) = h\nu_L ,$$

$$E(+\tfrac{1}{2}\leftrightarrow+\tfrac{3}{2}) = h(\nu_L - \nu_Q/2) ,$$

and

$$E(-\tfrac{3}{2}\leftrightarrow-\tfrac{1}{2}) = h(\nu_L + \nu_Q/2) ,$$

where the quadrupole coupling ν_Q is defined by $\nu_Q = e^2qQ/h$. Consequently, single-quantum transitions are expected to occur at the Larmor frequency, as in the pure Zeeman case, and also at frequencies symmetrically displaced above and below the Larmor frequency by an amount equal to $\nu_Q/2$. The expected variation in β asymmetry as a function of the perturbing field frequency is illustrated on the right-hand side of Fig. 2(b).

If these resonant frequencies are measured and if the EFG is known, the magnitude, but not the sign, of the quadrupole moment Q may be deduced. To determine the sign of Q, one would also need to know the sign of ν_Q, or, equivalently, whether the transition that occurs at the lowest resonant frequency (for example) involved the $(+\frac{3}{2},+\frac{1}{2})$ or the $(-\frac{3}{2},-\frac{1}{2})$ substates. The depolarization technique employed in this experiment is incapable of permitting the necessary distinction.

Besides single-quantum transitions, multiple-quantum transitions (MQT) are also possible. These connect initial and final states whose magnetic quantum numbers differ by more than unity, and they have been observed in a variety of resonant systems, including atomic and molecular beam resonance,[35,36] classical NMR,[37] and β-NMR.[38,39] The most probable MQT are two-quantum transitions, which occur between substates whose magnetic quantum numbers differ by 2, as, for example, between the $m=-\frac{3}{2}$ $(-\frac{1}{2})$ and $m=+\frac{1}{2}$ $(\frac{3}{2})$ substates of a nucleus with $J=\frac{3}{2}$. If the perturbing field applied contains just one frequency component, the transition energy must be supplied equally by the two quanta involved, and the resulting condition for resonance is $2h\nu=\Delta E$ $(m\leftrightarrow m+2)$. For $J=\frac{3}{2}$, the corresponding resonant frequencies lie midway between the central and extreme single-quantum frequencies, i.e., at $\nu=\nu_L\pm\nu_Q/4$ for $\theta=0°$.

The transition probability for such two-quantum transitions has been calculated, for the conditions under which the present measurements were made, using second-order perturbation theory.[25] The result indicates that these transitions should be well saturated, so that changes in the β symmetry whose magnitudes depend only on the initial substate populations should be observed at these additional perturbing field frequencies. These observations will then provide an additional measurement of the quadrupole coupling ν_Q.

To summarize the basic principles of the method, oriented nuclei in the state of interest are subjected to combinations of electric and magnetic fields whose influence on the magnetic substate energies can be calculated in terms of the nuclear moments of the state and the properties of the fields themselves. These substate energies in turn determine the resonant frequencies at which transitions between the substates may be induced by an applied perturbing field. Such transitions alter the substate populations, changing the polarization of the sample and the resulting β asymmetry. The resonant frequencies are determined experimentally by measuring the β asymmetry as a function of the perturbing field frequency, and from these frequencies values of the nuclear moments are deduced.

III. EXPERIMENTAL APPARATUS AND PROCEDURE

A. General description

The experiments were performed at the Los Alamos National Laboratory Van de Graaff Facility[40] using the Lamb-shift polarized triton source, the model FN tandem electrostatic accelerator, and the SDS-930 on-line data acquisition computer system. Polarized tritons, with their spins oriented vertically either up or down, were used to bombard the ^{7}Li-bearing targets in a specially-constructed, disk-shaped vacuum chamber positioned between the poles of a Varian NMR electromagnet, which produced a static, vertical magnetic field H_0. A general view of the target, chamber, and detectors is shown in Fig. 3.

To reduce background from prompt events, the triton beam was repetitively pulsed using an electrostatic deflector; each beam-on-target period of 200 ms was followed by a beam-off period of 300 ms. A weak oscillatory perturbing field, produced with a pair of small coils in nearly the Helmholtz configuration, was applied over the volume of the recoil-stopping material throughout each beam-on period and for 15 ms afterwards. Decay electrons originating from the product nuclei left the target chamber through thin Cu windows positioned above and below the recoil stopper and were counted in solid-state detector telescopes during the remaining 285 ms of the beam-off period. The frequency of the perturbing field was incremented by a fixed amount each time a predetermined number of beam-on/beam-off cycles was completed, until the desired range of frequencies was covered. This usually required 2–3 min. When a complete frequency scan had been performed with incident tritons of one spin state, the spin was reversed at the ion source, and the entire process was repeated, starting with the lowest perturbing frequency. Each experiment consisted of many such frequency

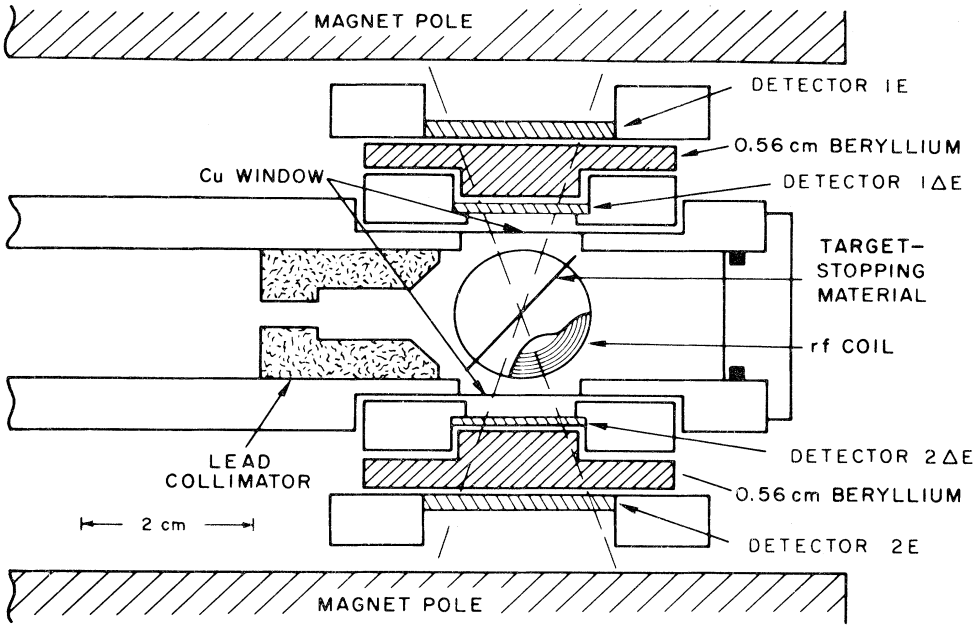

FIG. 3. Cross-sectional side view of the target chamber and detectors in place between the magnet pole pieces.

scans, so this procedure helped to ensure that drifts in any part of the system were averaged out over the duration of the run. Counts from the upper and lower detector telescopes were stored in separate sections of the computer memory for each frequency of the applied field and for each spin state of the incident beam. These data were used to compute the experimentally observed β asymmetry as a function of frequency, from which the values of the nuclear moments were to be deduced.

B. Experimental details

1. Polarized triton beam

A detailed description of the LANL Lamb-shift polarized triton source has been published elsewhere.[41,42] This source is generally capable of providing beam currents on target in excess of 100 nA, but for the present experiments peak beam currents of 30—40 nA provided satisfactory data rates. Beam polarizations were determined using the quench ratio method,[43] and average polarizations of 0.8 were observed throughout the runs.

Two considerations influenced the choice of incident beam energy. On one hand, the energy should be far enough above the ^{7}Li(t,p)^{9}Li reaction threshold to ensure a good production rate; on the other hand, the energy should be low enough to suppress the production of either ^{9}Li in excited states or other β-unstable nuclides.

Excitation functions for the ^{7}Li(t,p)^{9}Li and ^{6}Li(t,p)^{8}Li reactions have been measured[44] by Abramovich *et al.* for incident triton energies in the 2—7 MeV range. They found that the ^{9}Li yield rises fairly steeply for energies above the ^{7}Li(t,p) reaction threshold at 3.43 MeV and reaches a maximum at a triton energy near 5.5 MeV. For bombarding energies above 6.04 MeV, they also observed β activity from ^{8}Li produced in the ^{7}Li(t,d) reaction. Because such activity would create a particularly undesirable background in the present experiments, it was decided to keep the triton beam energy below 6 MeV. This restriction also ensured the ^{9}Li nuclei would be produced only in the ground state, because tritons of approximately 7.3 MeV energy are needed to reach the first excited state. Resonance scans were actually performed using tritons of 5.0, 5.4, and 5.5 MeV incident energy.

2. Targets and recoil stoppers

Two different types of target-recoil-stopper combinations were used in measuring the magnetic dipole and electric quadrupole moments. For the dipole moment studies, thin layers of isotopically enriched ^{7}Li evaporated on Au foils were employed: The enhanced isotopic abundance of ^{7}Li was greater than 99.99%, the areal density of the target layer was approximately 150 μg/cm^2, and the thickness of the Au backing foil, in which the ^{9}Li recoil nuclei were stopped, was 0.025 mm. Thick single crystals of $LiNbO_3$ were used in the quadrupole moment studies. These crystals, obtained commercially,[45] were approximately 1-mm thick, contained ^{7}Li and ^{6}Li nuclei in the ratio of their natural abundances (approximately 92.5% ^{7}Li to 7.5% ^{6}Li), and were oriented by the supplier so that the crystalline c axis made a 45° angle with respect to the crystal surface. This orientation was confirmed independently by x-ray diffraction measurements. During the experiments, the $LiNbO_3$ crystals were mounted so that the surface was at 45° with respect to the vertical direction and the c axis was aligned with the vertical magnetic field H_0.

3. Detectors and electronics

Electrons originating from the ^{9}Li decays were detected in two identical counter telescopes, one positioned directly

above the recoil-stopping material and one directly below it in such a way that the up/down asymmetry ratio $N(0°)/N(180°)$ could be measured. Each telescope contained a 500-μm thick, totally depleted surface barrier detector with 200-mm^2 active area, a 2-mm-thick Si(Li) detector with 500-mm^2 active area, and a 0.56-cm-thick Be disk placed between the detectors to stop low-energy electrons and other charged particles. Signals from the detectors were processed using standard charge-sensitive preamplifiers, linear amplifiers, timing single channel analyzers, and overlap coincidence units. A block diagram of the electronics is shown in Fig. 4.

Two conditions had to be satisfied to record a single event in either telescope: coincident pulses above single channel analyzer (SCA) thresholds must have been registered in both detectors of that telescope, and a special gating signal indicating that the counting period had begun had to be present. Because an electron required at least 2.2 MeV to penetrate the 500-μm surface barrier detector and 0.56-cm Be disk, electrons with lower energies could not reach the 2-mm detector to satisfy the coincidence requirement. On the other hand, most of the electrons originating from the ^{9}Li could do so, since the β end point energies for the two major decay branches are 13.5 and 11.0 MeV.[28] These conditions ensured good sensitivity for the events of interest while suppressing the copious background.

During the experiments, the sum of the counting rates in the two telescopes was typically 3×10^3 s^{-1} for 20 nA of 5.4 MeV tritons incident on the ^{7}Li target. Under similar conditions, but with the $LiNbO_3$ target, the rate was typically 10^4 s^{-1}. Singles rates in the detectors were usually a factor of 10 higher than these coincidence rates.

4. *Static magnetic field*

The vertical, static magnetic field H_0 was produced using a Varian-type V3401 NMR electromagnet with 22.9-cm-diam circular pole faces and a 10.2-cm gap. An NMR fluxmeter was used to map the field of this magnet, and it was found that, for central field strengths near 1 kG, the field homogeneity over the volume of the recoil-stopping material was better than 1 part in 10^4. The same fluxmeter, with its probe attached to the outer wall of the target chamber, was used to measure the field strength during the resonance experiments. A small correction was later applied to this measured field strength to account for the fact that the probe was necessarily slightly displaced from the actual position of the stopping material. Generally, values of H_0 very near 1 kG were employed in the resonance experiments, and the total uncertainty in their measurement was estimated to be 2.5 parts in 10^4.

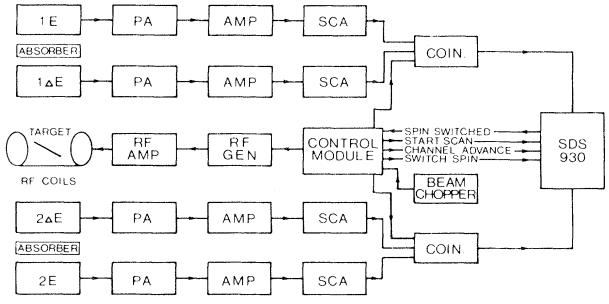

FIG. 4. Block diagram of the electronics used for data acquisition and experiment control. (PA is the preamplifier, AMP is the linear amplifier, SCA is the timing single channel analyzer, and COIN is the overlap coincidence unit.)

5. *Perturbing field*

The oscillatory perturbing field H_1 was generated using two small coils connected in series and positioned symmetrically to the right and left of the recoil stopper (as viewed by the incident beam) in nearly the Helmholtz configuration. The driving signal for these coils was an amplified sine wave obtained from a General Radio Corporation-type 1164A Coherent Decade Frequency Synthesizer, whose digitally selected output frequency was accurate to 1 part in 10^6, could be remotely programmed, and could be frequency modulated, if desired. During the experiments, the rms current through the coils was approximately 250 mA; the amplitude of H_1 at the center of the recoil stopper (i.e., midway between the coils and on their common axis) was then about 2.5 G.

IV. RESULTS AND DISCUSSION

A. Yield purity and off-resonance β asymmetry

Before the resonance experiments were begun, several checks were made to verify the desired ^{9}Li nuclei could be produced without significant amounts of unwanted background and that their net polarization would be large enough to provide a measurable β asymmetry.

The purity of the reaction yield was assessed by multiscaling the β activity created in the triton bombardment of the ^{7}Li and $LiNbO_3$ targets and comparing the observed half-life with the known half-life of ^{9}Li. Typical results obtained for 5.4 MeV incident tritons are shown in Fig. 5, where the solid lines are included for reference and represent the expected ^{9}Li decay rate. Very good agreement with this expected rate was observed using the enriched ^{7}Li targets, indicating that ^{9}Li was the major short-lived β activity present. By contrast, the results of the $LiNbO_3$ measurements implied the additional existence of some longer-lived activity, possibly from ^{8}Li ($T_{1/2}=0.84$ s) produced in the exoergic ^{6}Li(t,d) reaction on the ^{6}Li nuclei present in the crystals. The multiscaling periods were too short to permit a definite identification of the responsible nuclide(s); nor could their concentration relative to ^{9}Li be estimated precisely. Nevertheless, the ^{9}Li yield was considered adequate for the resonance experiments.

Off-resonance β-asymmetry measurements were made using incident tritons of several energies between 5.0 and 6.0 MeV. The procedure was essentially the one that would be used in the later resonance scans, except that the perturbing field was turned off. Small asymmetries, nearly independent of the bombarding energy, were observed with both types of target. Typical values were $-0.007(1)$ for the ^{7}Li targets and $-0.0030(5)$ for the $LiNbO_3$ crystals. To verify that these measured asymmetries were re-

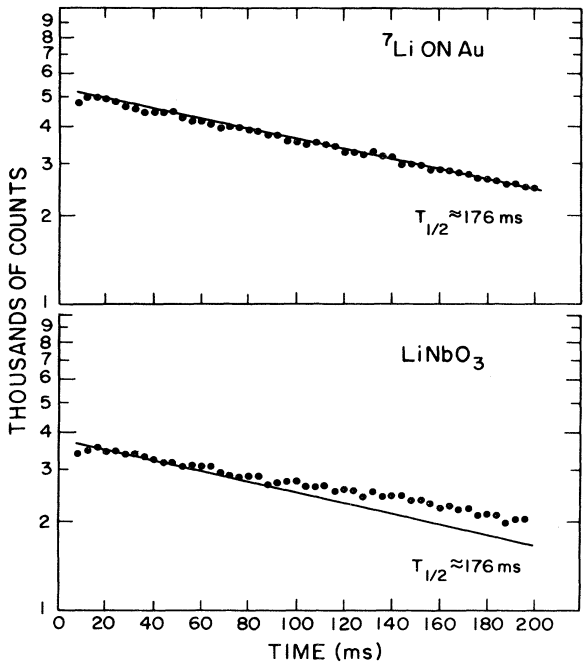

FIG. 5. Multiscaled β activity observed for 5.4-MeV tritons incident on (a) enriched ^{7}Li layers with Au backings and (b) thick $LiNbO_3$ single crystals. For comparison, the expected decay rate of ^{9}Li ($T_{1/2}=0.176$ s) is indicated by a solid line.

lated to the nuclear polarization of the ^{9}Li recoils and were not simply instrumental in origin, the measurements were repeated with unpolarized tritons, and asymmetries consistent with zero were observed.

From these measured asymmetries and from the calculated effective asymmetry parameter A_{eff}, lower limits on the average nuclear polarizations obtained with these targets may be deduced. For the ^{7}Li target, this polarization is $+0.071(19)$, whereas for the $LiNbO_3$ target, the result is $+0.031(9)$. It is possible that a larger nuclear polarization was actually obtained when the ^{7}Li target was used, but a more plausible explanation for the smaller asymmetries observed with the $LiNbO_3$ targets is that a larger fraction of the ^{9}Li nuclei lost their polarization while coming to rest in those crystals than in the Au stoppers. These nuclei would then constitute, in effect, an unpolarized background activity. The positive polarizations observed with both types of target imply that the net spin orientation of the ^{9}Li nuclei produced in the ^{7}Li($\vec{t}$,p) reaction was parallel to that of the incident triton beam. Similar results have been reported[22] for other reactions used in β-NMR experiments.

B. ^{9}Li dipole moment measurements

Resonance experiments using the enriched ^{7}Li targets on the Au recoil-stopping foils were performed with polarized tritons of 5.0, 5.4, and 5.5 MeV incident energy. For two of the experiments, the strength of the static magnetic field was fixed at one value; for the third, it was changed slightly to verify that the ^{9}Li Larmor frequency also changed in the proper manner.

Initial frequency scans were performed in rather coarse frequency steps of 10 kHz, with a 5-kHz modulation; once evidence of resonant depolarization had been observed, finer scans were performed with frequency steps of 1 kHz and no modulation. The results of three such scans are presented in Fig. 6. Gaussian line shapes, represented in the figure by solid lines, were fitted to the data in order to extract the resonant frequencies. Because the central frequencies were the only features of the resonance lines needed to compute a value for the dipole moment, no attempt was made to derive and fit a more realistic line shape. Nevertheless, at least qualitative information may be deduced from the other properties of the fitted lines. For example, each of the lines is reasonably narrow, which imples that those ^{9}Li nuclei whose polarization was preserved during the implantation process found well-defined stopping sites where the EFG's were indeed small or absent. Further, because the β asymmetry falls nearly to zero at the center of each line, it is evident that the ^{9}Li nuclear polarization was almost completely destroyed by the perturbing field at the Larmor frequency.

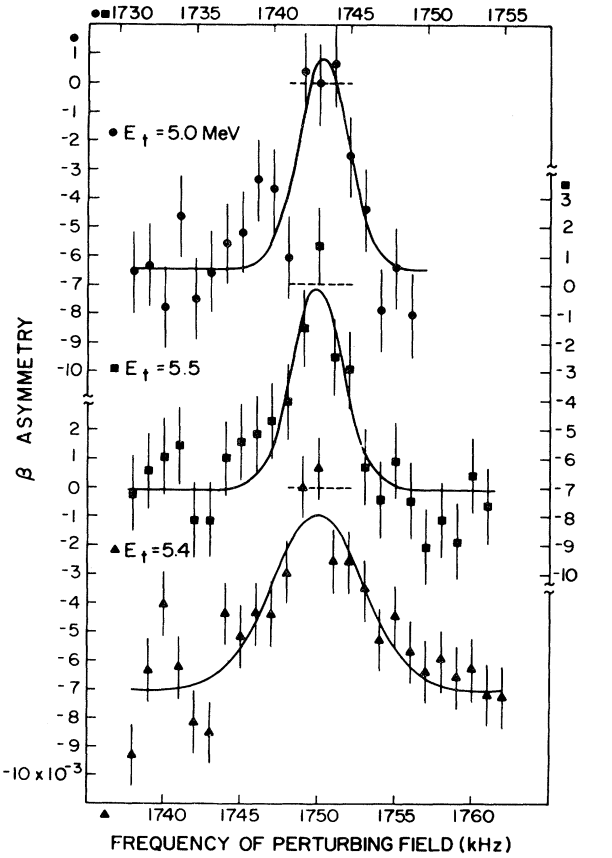

FIG. 6. Measured β asymmetry versus frequency of the perturbing field for enriched ^{7}Li targets on Au backings. Data are shown for three triton bombarding energies, and each set of data should be referred to the vertical and horizontal scales marked with the appropriate plotting symbol. The solid lines represent Gaussian line shapes fitted to the data in order to extract the resonant frequencies.

TABLE II. Results of β-NMR measurements on ^{9}Li nuclei implanted in Au.

	(a)	(b)	(c)
Triton energy (MeV)	5.0	5.5	5.4
Proton Larmor frequency in external field H_0 (MHz)	4.2458(12)	4.2458(12)	4.2634(12)
Amplitude H_1 of perturbing field (G)	2.0	2.0	1.8
Off-resonance asymmetry[a]	−0.0065(1)	−0.0071(1)	−0.0070(1)
Height of resonance line[a]	0.0073(5)	0.0069(4)	0.0061(1)
Width (FWHM, kHz)[a]	3.8(4)	4.2(3)	7.0(1)
^{9}Li Larmor frequency in external field H_0 (MHz)[a]	1.7432(2)	1.7428(3)	1.7500(2)
χ^2/n[a]	1.14	1.12	1.05
^{9}Li g factor	2.2933(7)	2.2927(8)	2.2927(7)

[a]Derived from computer fits.

The deduced Larmor frequency for each run is listed in Table II together with the measured proton resonant frequency in the static field H_0 and other relevant parameters. Quantities in the table that are marked with a superscript were derived from the computer fits. For each case, the ratio of the ^{9}Li g factor to that of the proton was computed from the measured Larmor frequencies using the relation

$$|g(^9\mathrm{Li})/g(^1\mathrm{H})| = \nu_L(^9\mathrm{Li})/\nu_L(^1\mathrm{H}) .$$

The value of the proton g factor used in the calculations was[46]

$$g(^1\mathrm{H}) = 5.585\,552(62) ,$$

and the weighted average of the ^{9}Li g factors deduced from the measurements was

$$|g(^9\mathrm{Li})_{\mathrm{uncorr}}| = 2.2929(4) .$$

Multiplying this result by the spin of the ^{9}Li ground state yields the desired dipole moment:

$$|\mu(^9\mathrm{Li})_{\mathrm{uncorr}}| = 3.4394(6)\,\mu_N .$$

Two small corrections must be applied to this value to account for the fact that the magnetic field acting on the ^{9}Li nuclei differed slightly from the field measured by the proton resonance probe, even after allowance had been made for possible physical displacements. The effective field H_{eff} at a ^{9}Li nucleus implanted in a Au recoil stopper may be related to the external field H_0 by

$$H_{\mathrm{eff}} = H_0(1-\sigma+K) ,$$

where σ is the diamagnetic shielding factor and K is the Knight shift.

Diamagnetic shielding occurs because the external field induces current densities in the closed shells of atomic electrons surrounding the implanted Li ion, which in turn produce a magnetic field that is proportional in magnitude but opposite in direction to the applied field. The shielding factor for the Li^+ ion has been calculated by Feiock and Johnson using relativistic Hartree-Fock-Slater theory; it value[47] is

$$\sigma(\mathrm{Li}^+) = 0.000\,095\,53 ,$$

and its uncertainty[48] is about 5% of that value.

The Knight shift arises because of interactions involving the conduction electrons in the metal host. Its value for ^{9}Li in Au has not been measured or calculated; however, Haskell and Madansky estimated the Knight shift for ^{8}Li nuclei implanted in Au foils from measurements of the ^{8}Li spin-lattice relaxation time. Their result,[10]

$$K(^8\mathrm{Li\ in\ Au}) \approx 0.000\,17(7) ,$$

should also represent a good estimate of the shift for ^{9}Li nuclei in Au.

Because the dipole moment deduced from this type of measurement is inversely proportional to the strength of the magnetic field acting at the nucleus, the correction that must be applied to the computed moment takes the form

$$\mu_{\mathrm{corr}} = \mu_{\mathrm{uncorr}}/(1-\sigma+K) .$$

Inserting the proper values for σ and K yields the final result

$$|\mu(^9\mathrm{Li})_{\mathrm{corr}}| = 3.4391(6)\,\mu_N .$$

C. ^{9}Li quadrupole moment measurements

Resonance experiments were also performed using the thick $LiNbO_3$ targets and polarized tritons of 5.4 and 5.5 MeV incident energy. The resonance scans were done in steps of 1 kHz, with no modulation, and covered a range of perturbing field frequencies that extended approximately 50 kHz above and below the calculated Larmor frequency. During the subsequent analysis, the counts in each group of three successive 1-kHz bins were added together to improve statistics.

Results of two sets of measurements are presented in Fig. 7. For each set, the $LiNbO_3$ crystal was oriented so that its c axis was parallel to the direction of the applied magnetic field. The data shown in part (a) of the figure were obtained first and with the crystals as supplied by the manufacturer (etched after cutting, to remove surface damage); those in part (b) were obtained later, after the crystal surfaces had been ground with 12.5-μm AlO powder. It is evident that the two sets of data do not have the same shape. In particular, some of the structure apparent in part (a) is missing in part (b), and the latter data

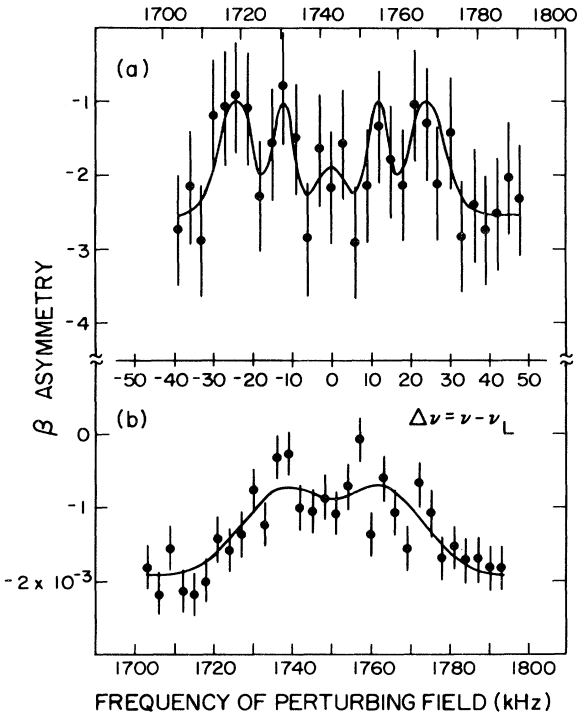

FIG. 7. Measured β asymmetry versus frequency of the perturbing field for thick $LiNbO_3$ single crystals oriented with their c axes parallel to the external magnetic field. Data in (a) were taken with crystals as supplied by the manufacturer, those in (b) were taken after the crystal surfaces were ground with 12.5-μm AlO powder. The solid line in (a) represents a fit to five Gaussian line shapes; that in (b) represents a fit to two Gaussians and serves only to guide the eye.

were not used in determining the quadrupole coupling.

After some consideration, it became clear that the surface grinding was reponsible for the difference between the two sets of data. This grinding was done to remove material near the surface of the crystals that darkened as a result of the triton bombardment during the first experiments. The darkening was believed to be an indication of radiation damage to the crystal lattice, which might cause rapid depolarization of the implanted nuclei. It was later recognized that the grinding itself probably produced a layer of damaged material whose thickness may have been as much as twice the diameter of the abrasive used,[49] or about 25 μm. Calculations based on the stopping-power tables of Northcliffe and Schilling[50] indicated that as many as 90% of the ^{9}Li nuclei would have stopped in such a layer, and those nuclei would not have experienced the EFG distribution characteristic of single-crystal $LiNbO_3$. These observations emphasize the importance of proper surface treatment for crystals used in experiments of this type, and suggest that methods other than grinding, such as annealing, would be more appropriate for dealing with radiation-damaged crystals.

The data presented in Fig. 7(a) were fitted by computer to an expression containing five Gaussian resonance lines, in order to extract the resonant frequencies for the various possible one- and two-quantum transitions. Although a method for deriving a theoretically exact line shape has been described by Dubbers,[51] this more sophisticated approach was not used. The quantities determined by the fitting program were the position of the central line (the Larmor frequency), the splitting between the central line and each of the outer lines, and the splitting between the central line and each of the inner lines. Additionally, the heights and widths of the lines were found, subject to several constraints: (1) the widths of the central line and the outer lines were constrained to be the same, since all three linese were interpreted as single-quantum resonances; (2) the common width of the inner line was allowed to be different from that of the outer lines, in keeping with the assumption that the inner lines represented two-quantum resonances; (3) the heights of the outer lines were constrained to be equal, as were the heights of the inner lines; (4) the height of the central line was allowed to vary independently. In Table III the best values of these parameters are listed together with other relevant data concerning the measurement; the entries marked with a superscript represent values determined by the fitting program.

Several points can be made concerning the results of the fitting procedure. First, the deduced Larmor frequency for ^{9}Li in $LiNbO_3$ agrees with the frequency previously measured in Au for the same magnetic field strength H_0. Second, the splitting between the central line and each of the outer lines is twice as large as the splitting between the central line and each of the inner lines, which is consistent with the assumption that the outer and inner lines represent one- and two-quantum transitions, respectively. Third, the width of the inner lines is apparently about one-half that of the outer lines, which is also consistent[52] with that assumption, although the uncertainties in the fitted line widths are fairly large. Fourth, the deduced width of the outer lines, ≈ 10 kHz, is reasonable in the sense that it is close to the value of ≈ 9 kHz measured by Halstead[33] for the room-temperature width of the quadrupole shifted resonance lines of ^{7}Li in $LiNbO_3$. Finally, the shape of the fitted asymmetry spectrum, which is shown as a solid line in Fig. 7(a), is similar to the result of an exact line shape calculation,[51] including multiple quantum resonances, for the case of $J = \frac{3}{2}$. This similarity supports the earlier conclusion that the two-quantum transitions in this

TABLE III. Results of β-NMR measurements on ^{9}Li nuclei in $LiNbO_3$.

Triton energy (MeV)	5.5
Proton Larmor frequency in external field H_0 (MHz)[a]	4.2458(12)
Amplitude H_1 of perturbing field (G)	2.5
Off-resonance asymmetry[a]	−0.025(3)
^{9}Li Larmor frequency in external field H_0 (MHz)	1.7429(10)
Height of outer lines[a]	0.0015(5)
Width of outer lines (FWHM, kHz)[a]	10.0(32)
Splitting of outer lines (kHz)[a]	24.2(15)
Height of inner lines[a]	0.0015(6)
Width of inner lines (FWHM, kHz)[a]	5.1(21)
Splitting of inner lines[a]	12.1(10)
Height of central line[a]	0.0006(6)
χ^2/n	0.33

[a]Determined by the fitting program.

system should be saturated by the relatively strong perturbing field applied. The relative heights of the resonance lines further suggests that the initial populations of the two $|m|=\frac{1}{2}$ substates were not very different, whereas the population differences between the $|m|=\frac{3}{2}$ and the neighboring $|m|=\frac{1}{2}$ substates were greater.

The separation of the outer resonance lines implies a quadrupole coupling for ^{9}Li in $LiNbO_3$ equal to

$$|\nu_Q| = 2\times(24.2\pm1.5\text{ kHz}) = 48.4\pm3.0\text{ kHz}\ .$$

Similarly, the separation of the inner lines implies that

$$|\nu_Q| = 4\times(12.1\pm1.0\text{ kHz}) = 48.4\pm4.0\text{ kHz}\ .$$

The weighted average of these results is

$$|\nu_Q(^9\text{Li in LiNbO}_3)| = 48.4\pm2.4\text{ kHz}\ .$$

In order to evaluate the ^{9}Li quadrupole moment using this quadrupole coupling, the magnitude of the EFG at the stopping site of the implanted nucleus must be determined. Several methods have been employed in similar cases to calculate or measure the necessary field gradient, but serious difficulties are associated with most of them. The most reliable method, when it can be applied, seems to be to select as a recoil stopper a material that contains a stable isotope of the unstable nucleus under investigation and in which the quadrupole coupling of the stable isotope has been measured. If the quadrupole moment of the stable isotope is also known, and if the implanted nucleus can be assumed to replace its stable counterpart in the crystal lattice and thereby experience the same EFG, the ratio of the quadrupole couplings may then be taken to be equal to the ratio of the respective quadrupole moments.

In the present case, the ratio of the unknown quadrupole moment of ^{9}Li to the known moment of ^{7}Li is assumed to equal the ratio of the newly measured coupling of ^{9}Li in $LiNbO_3$ to the previously measured coupling of ^{7}Li in that crystal:

$$\left|\frac{Q(^9\text{Li})}{Q(^7\text{Li})}\right| = \frac{\nu_Q(^9\text{Li in LiNbO}_3)}{\nu_Q(^7\text{Li in LiNbO}_3)}\ .$$

Because the β-NMR method as employed in the present experiments measures only the magnitude of the quadrupole coupling, and not its sign, only the absolute value of the quadrupole moment ratio can be determined.

Clearly, the fundamental assumption on which the validity of this procedure depends is that the implanted nucleus occupies a position equivalent to that of one of its stable counterparts and interacts with the same EFG. It is not obvious that this is a good assumption, but it can be tested experimentally in the following way. The quadrupole coupling of the unstable nucleus may be measured in a number of different compounds, each of which contains the same stable isotope of the proper element. The ratio of the coupling of the two isotopes in each of the compounds may then be compared and, if the ratios agree it may be concluded that the implanted nucleus did in fact replace one of its stable partners in each case.

This test has not been performed for ^{9}Li, but similar tests have been carried out for ^{8}Li and ^{12}B nuclei implanted in material that contained an appropriate stable isotope, either ^{7}Li or ^{11}B; the results appear in Table IV. All of the measurements involving lithium nuclei were performed using single crystal hosts; most of the ones involving boron nuclei were performed using powder samples. Only the smaller of the two couplings listed for ^{12}B in ZrB_2 was measured in a single crystal.

TABLE IV. Quadrupole couplings of stable and unstable isotopes of the same element in different compounds.

Stopping Material	$LiIO_3$[a]	$LiNbO_3$[b]	$LiTaO_3$[c]
$\nu_Q(^8\text{Li})$ (kHz)	29.2(8)	43(3)	60.2(3)
$\nu_Q(^7\text{Li})$ (kHz)	44(3)	54.5(5)	77.6(5)
$\nu_Q(^8\text{Li})/\nu_Q(^7\text{Li})$	0.66(5)	0.79(6)	0.78(1)
Stopping material	TiB_2[d]	ZrB_2[e]	ZrB_2[f]
$\nu_Q(^{12}\text{B})$ (kHz)	154(16)	49(5)	38.7(11)
$\nu_Q(^{11}\text{B})$ (kHz)	360(20)	118(10)	118(10)
$\nu_Q(^{12}\text{B})/\nu_Q(^{11}\text{B})$	0.43(5)	0.41(5)	0.33(3)

[a]Reference 23.
[b]Reference 53.
[c]Reference 39.
[d]Reference 54.
[e]Reference 54.
[f]Reference 55.

These results demonstrate that fair agreement exists between the ratios of the quadrupole couplings measured in different materials. They suggest, however, that if a quadrupole moment ratio is derived on the basis of couplings measured in just one compound, it may differ from the results of measurements made in other compounds by as much as 20%. Since the quadrupole moments of the nuclei involved do not change, the assumption that equal field gradients act on both the implanted nucleus and the stable nucleus it is supposed to replace must not be trusted completely.

With this consideration in mind, the couplings of ^{9}Li and ^{7}Li in $LiNbO_3$ may be compared in order to obtain an estimate of the ^{9}Li quadrupole moment. Two measurements of the ^{7}Li coupling have been made using conventional NMR techniques[32,33]; the average of the results is

$$\nu_Q(^7\text{Li in LiNbO}_3) = 54.7\pm0.3\text{ kHz}\ .$$

The ratio of the respective quadrupole moments is then approximately equal to

$$\left|\frac{Q(^9\text{Li})}{Q(^7\text{Li})}\right| = \frac{\nu_Q(^9\text{Li in LiNbO}_3)}{\nu_Q(^7\text{Li in LiNbO}_3)} = \frac{48.4\pm2.4\text{ kHz}}{54.7\pm0.3\text{ kHz}} = 0.88\pm0.04\ .$$

The quoted uncertainty does not reflect the sizable systematic errors ($\simeq$20%) that may arise in connection with the procedure used to estimate the EFG at the nucleus. If these errors are included, the quadrupole-moment ratio should be given as

$$\left|\frac{Q(^9\text{Li})}{Q(^7\text{Li})}\right| = 0.88\pm0.18\ .$$

The quadrupole moment of ^{7}Li is known from molecular-beam measurements and from optical double-

resonance studies; the weighted average of two recent values[56,57] is

$$Q(^7\text{Li}) = -36.6 \pm 0.3 \text{ mb} .$$

In combination with the measured ratio of the respective couplings, this implies

$$|Q(^9\text{Li})| = 32.2 \pm 6.6 \text{ mb} .$$

D. Comparison with shell-model calculations

It is of interest to compare the experimental values of the ^{9}Li ground-state moments with the results of appropriate nuclear structure calculations. Cohen and Kurath[58] and Barker[59] have made extensive shell model studies of the 1-p shell nuclei ($5 \leq A \leq 16$) in which they deduced values for the matrix elements of the two-body effective interactions between the p-shell valence nucleons by fitting experimental data on selected states in those nuclei. For simplicity, they made the usual assumptions that the $1s^4$ (^{4}He) core is inert and undistorted, and that the states they fitted were well described by the lowest shell-model configurations consistent with their observed spins and parities. Using the wave functions they extracted for these and other states, they were then able to compute values for various observables of interest, such as electromagnetic moments and transition probabilities.

In Table V, the measured values of the ^{7}Li and ^{9}Li ground-state moments are compared with values calculated using wave functions of Cohen and Kurath[60] and those of Barker.[61] Two predictions for each quantity are attributed to Cohen and Kurath; they resulted from making slightly different assumptions about the form of the two-body matrix elements, and the original description of the calculation[58] should be consulted for more details. It is evident that the measured ^{9}Li dipole moment is in good agreement with all of the calculated values, which bracket it and differ from it by at most 3%.

Comparison of the measured and calculated quadrupole moments requires some explanation. First, it should be observed that the shell model predicts quadrupole moment values for both ^{9}Li and ^{7}Li that are smaller than the measured ones. This is a well-known characteristic of calculations in which core deformation and configuration mixing have been neglected.[62,63] It is also well known that the values of the quadrupole moments and of certain $E2$ transition probabilities so calculated can be "enhanced," or brought into better agreement with the typically larger experimental values, by attributing a phenomenological "effective charge" to each of the valence nucleons.[64] These effective charges compensate to some extent for the collective effects that are omitted from the simplest shell-model calculations.

In one common formulation, the effective charge is assumed to be an isoscalar; that is, the additional charges attributed to the valence protons and neutrons are assumed to be equal. Then, the effective charges of those nucleons are

$$e_p = (1+\delta)e$$

and

$$e_n = \delta e ,$$

where δ is the additional charge. Several analyses[64,65] have shown that, for p-shell nuclei, reasonable agreement between the measured and calculated quadrupole moments and $E2$ probabilities can be obtained for $\delta \simeq 0.5$.

While the introduction of effective charges generally increases the calculated quadrupole moments, the extent to which this occurs is different for different nuclear states. This is shown explicitly in Barker's expression for the quadrupole moment ratio $Q(^9\text{Li})/Q(^7\text{Li})$, presented in Table V. If the additional charge, δ, is taken to be 0.5 for valence nucleons in both ^{9}Li and ^{7}Li, and if the mean-square charge radius $\langle r^2 \rangle$ of ^{9}Li is assumed to be equal to that of ^{7}Li, that expression yields

$$Q(^9\text{Li})/Q(^7\text{Li}) = 1.06 .$$

Kurath estimated[60] that the ratio of enhanced moments should be in the range 0.8—0.9. He also noted that the experimental values of the ground-state quadrupole moments, taken alone, suggest that a smaller value of δ seems needed for ^{9}Li than for ^{8}Li or ^{7}Li. In any case, since the measured ratio

$$|Q(^9\text{Li})/Q(^7\text{Li}) = 0.88 \pm 0.18$$

contains an uncertainty of 20% due to the assumptions made in evaluating the EFG, the shell-model predictions are considered to be in satisfactory agreement with the experimental result.

TABLE V. Comparison of measured ^{7}Li and ^{9}Li ground-state moments with shell model predictions.

	$\mu(^9\text{Li})$ μ_N	$\mu(^7\text{Li})$ μ_N	$Q(^9\text{Li})$ mb	$Q(^7\text{Li})$ mb	$Q(^9\text{Li})/Q(^7\text{(Li)}$
Kurath					
6—16 2BME	3.3753	3.1703	−22.91	−17.50	1.31
8—16 POT	3.4832	3.2608	−24.09	−19.16	1.26
Barker	3.401	3.11			$1.305 \frac{1+2.02\,\delta(^9\text{Li})}{1+2.95\,\delta(^7\text{Li})} \frac{\langle r^2 \rangle_9}{\langle r^2 \rangle_7}$
Experiment	±3.4391(6)	3.256424(2)[a]	±32.2(66)	−36.6(3)[b]	±0.88(18)

[a]Reference 46.
[b]Reference 56.

V. CONCLUSION

The (t,p) reaction, initiated by polarized tritons, has been shown to be suitable for producing and polarizing short-lived nuclei for study using the β-NMR technique. The ground-state electromagnetic moments of ^{9}Li have been measured in this way, and their values have been found to be in reasonable agreement with shell-model predictions.

ACKNOWLEDGMENTS

F.D.C. and L.M. wish to acknowledge the hospitality and assistance of the personnel at the Los Alamos Van de Graaff Facility, and in particular, the kind help of Judy Gursky, who made the enriched ^{7}Li targets. F. D. C. wishes to thank his friends, Joseph A. McClintock, A. J. Caffrey III, David A. Stromswold, and Don O. Elliott, for their considerable help in running the experiments. This work was performed under the auspices of the United States Department of Energy.

---

*Present address: Physics Department, United States Naval Academy, Annapolis, MD 21402.

[1]Donald Connor, Phys. Rev. Lett. 3, 429 (1959).

[2]T. Tsang and D. Connor, Phys. Rev. 132, 1141 (1963).

[3]H. Ackermann, D. Dubbers, M. Grupp, P. Heitjans, G. Zu Putlitz, and H.-J. Stöckmann, Phys. Lett. 41B, 143 (1972).

[4]H. Ackermann, Hyp. Int. 4, 645 (1978).

[5]L. F. Chase, Jr. and G. Igo, Phys. Rev. 116, 170 (1959).

[6]Kenzo Sugimoto, Akira Mizobuchi, Kozi Nakai, and Kozi Matuda, J. Phys. Soc. Jpn. 21, 213 (1966).

[7]J. J. Berlijn, P. W. Keaton, Jr., L. Madansky, George E. Owen, Loren Pfeiffer, and N. R. Roberson, Phys. Rev. 153, 1152 (1967).

[8]J. C. Wells, Jr., R. L. Williams, Jr., L. Pfeiffer, and L. Madansky, Phys. Lett. 27B, 448 (1968).

[9]Kenzo Sugimoto, Kozi Nakai, Kozi Matuda, and Tadanori Minamisono, J. Phys. Soc. Jpn. 25, 1258 (1968).

[10]R. C. Haskell and L. Madansky, Phys. Rev. C 7, 1277 (1973).

[11]T. Minamisono, Y. Nojiri, A. Mizobuchi, and K. Sugimoto, J. Phys. Soc. Jpn. 34 (suppl.), 156 (1973).

[12]R. L. Williams, Jr. and L. Madansky, Phys. Rev. C 3, 2149 (1971).

[13]K. Sugimoto, A. Mizobuchi, and T. Minamisono, in *Hyperfine Interactions in Excited Nuclei* (Gordon and Breach, New York, 1971), p. 325.

[14]K. Sugimoto, A. Mizobuchi, T. Minamisono, and Y. Nojiri, J. Phys. Soc. Jpn. 34 (suppl.), 158 (1973).

[15]E. W. Otten, in *Hyperfine Interactions in Excited Nuclei* (Gordon and Breach, New York, 1971), p. 363.

[16]Rainer Neugart, Z. Phys. 261, 237 (1973).

[17]M. Deimling, R. Neugart, and H. Schweickert, Z. Phys. A 273, 15 (1975).

[18]Eugene D. Commins and David A. Dobson, Phys. Rev. Lett. 10, 347 (1963).

[19]F. P. Calaprice, E. D. Commins, and D. A. Dobson, Phys. Rev. 137, B1453 (1965).

[20]J. W. Hugg, D. L. Clark, J. R. Hall, S. J. Freedman, B. B. Triplett, and S. S. Hanna, Bull. Am. Phys. Soc. 23, 953 (1978).

[21]T. Minamisono, J. W. Hugg, D. G. Mavis, T. K. Saylor, H. F. Glavish, and S. S. Hanna, Phys. Lett. 61B, 155 (1976).

[22]T. Minamisono, J. W. Hugg, J. R. Hall, D. G. Mavis, H. F. Glavish, and S. S. Hanna, Phys. Rev. C 14, 376 (1976).

[23]T. Minamisono, J. W. Hugg, D. G. Mavis, T. K. Saylor, S. M. Lazarus, H. F. Glavish, and S. S. Hanna, Phys. Rev. Lett. 34, 1465 (1975).

[24]J. W. Hugg, T. Minamisono, H. F. Glavish, and S. S. Hanna, Bull. Am. Phys. Soc. 20, 1495 (1975).

[25]Francis David Correll, Ph.D. thesis, The Johns Hopkins University, 1977.

[26]F. D. Correll, A. J. Caffrey III, D. O. Elliott, Jr., J. A. McClintock, L. Madansky, R. Hardekopf, and J. Sunier, Bull. Am. Phys. Soc. 21, 513 (1976).

[27]J. D. Jackson, S. B. Treiman, and H. W. Wyld, Jr., Phys. Rev. 106, 517 (1957).

[28]F. Ajzenberg-Selove, Nucl. Phys. A230, 114 (1979).

[29]Y. S. Chen, T. A. Tombrello, and R. W. Kavanaugh, Nucl. Phys. A146, 136 (1970).

[30]C. P. Slichter, *Principles of Magnetic Resonance* (Springer, Berlin, 1978), p. 3.

[31]H. D. Megaw, *Crystal Structures: A Working Approach* (Saunders, Philadelphia, 1973), pp. 223–241.

[32]G. E. Peterson, P. M. Bridenbaugh, and P. Green, J. Chem. Phys. 46, 4009 (1967).

[33]T. K. Halstead, J. Chem. Phys. 53, 3427 (1970).

[34]C. P. Slichter, *Principles of Magnetic Resonance* (Springer, Berlin, 1978), p. 289.

[35]V. W. Hughes and L. Grabner, Phys. Rev. 79, 314 (1950).

[36]P. Kusch, Phys. Rev. 93, 1022 (1954).

[37]W. A. Anderson, Phys. Rev. 104, 850 (1956).

[38]R. E. McDonald and T. K. McNab, Phys. Rev. Lett. 32, 1133 (1974).

[39]D. Dubbers, K. Dörr, H. Ackermann, F. Fujara, H. Grupp, M. Grupp, P. Heitjans, A. Körblein, and H.-J. Stöckmann, Z. Phys. A 282, 243 (1977).

[40]R. Woods, J. L. McKibben, and R. L. Henkel, Nucl. Instrum. Methods 122, 81 (1974).

[41]R. A. Hardekopf, in *Proceedings of the Fourth International Symposium on Polarization Phenomena in Nuclear Reactions,* edited by W. Grüebler and V. König (Birkhaüser, Basel, 1976), pp. 865–866.

[42]R. A. Hardekopf, G. G. Ohlsen, R. V. Poore, and Nelson Jarmie, Phys. Rev. C 13, 2127 (1976).

[43]G. G. Ohlsen, J. L. McKibben, G. P. Lawrence, P. W. Keaton, Jr., and D. D. Armstrong, Phys. Rev. Lett. 27, 599 (1971).

[44]S. N. Abramovich, B. Ya. Guzhovskii, A. G. Zvengorodskii, and S. V. Trusillo, Izv. Akad. Nauk SSR, Ser. Fiz. 37, No. 9, 1967 (1973) [Bull. Acad. Sci. USSR, Phys. Ser. 37, No. 9, 144 (1973)].

[45]Harshaw Chemical Company, Solon, OH 44139.

[46]G. H. Fuller and V. W. Cohen, Nucl. Data, Sect. A 5, 436 (1969).

[47]F. D. Feiock and W. R. Johnson, Phys. Rev. 187, 39 (1969).

[48]G. H. Fuller and V. W. Cohen, Nucl. Data, Sect. A 5, 437 (1969).

[49]G. Dearnaley and D. C. Northrup, *Semiconductor Counters for Nuclear Radiations* (Wiley, New York, 1963), p. 149.

[50]L. C. Northcliffe and R. F. Schilling, Nucl. Data, Sect. A 7, 233 (1970).

[51]Dirk Dubbers, Z. Phys. A 276, 245 (1976).

[52]Shaul Yatsiv, Phys. Rev. 113, 1522 (1959).

[53]H. Ackermann, D. Dubbers, M. Grupp, P. Heitjans, and H.-J. Stöckmann, Phys. Lett. 52B, 54 (1974).
[54]Tadanori Minamisono, Kozi Matuda, Akira Mizobuchi, and Kenzo Sugimoto, J. Phys. Soc. Jpn. 30, 311 (1971).
[55]T. Minamisono, S. Kogo, K. Okajima, and K. Sugimoto, Hyp. Int. 4, 224 (1978).
[56]Sheldon Green, Phys. Rev. A 4, 251 (1971).
[57]H. Orth, H. Ackermann, and E. W. Otten, Z. Phys. A 273, 221 (1975).
[58]S. Cohen and D. Kurath, Nucl. Phys. 73, 1 (1965).
[59]F. C. Barker, Nucl. Phys. 83, 418 (1966).
[60]Dieter Kurath (private communication).
[61]Frederick Barker (private communication).
[62]J. H. van der Merwe, Phys. Rev. 131, 2181 (1963).
[63]Dieter Kurath, Phys. Rev. 140, B1190 (1965).
[64]Denys H. Wilkinson, Comments Nucl. Part. Phys. 1, 139 (1967).
[65]E. K. Warburton, D. E. Alburger, D. H. Wilkinson, and J. M. Soper, Phys. Rev. 129, 2191 (1963).